Gary W. Slater[1]
Claude Desruisseaux[1]
Christine Villeneuve[1*]
Hong L. Guo[1]
Guy Drouin[2]

[1]**Department of Physics**
[2]**Department of Biology, University of Ottawa, Ottawa, Ontario**

Trapping gel electrophoresis of end-labeled DNA: An analytical model for mobility and diffusion

As shown by Ulanovsky, Drouin and Gilbert (*Nature* 1990, *343*, 190–192), the gel electrophoretic migration of DNA is severely reduced by steric trapping when streptavidin is attached to one end of the polyelectrolyte. We present a model that allows us to calculate both the mobility and the diffusion coefficient, hence the resolution factor of the resulting separation. We compare our results to those of Défontaines and Viovy (*Electrophoresis* 1993, *14*, 8–17) and we show that the averages over the molecular conformations must be done carefully. We also show that trapping increases diffusion substantially and that this makes constant-field trapping electrophoresis incapable of increasing the number of bases read per sequencing run. Finally, we conclude that severe trapping may lead to highly anomalous transport behavior where one cannot define a velocity or a diffusion constant.

1 Introduction

The separation mechanisms of DNA gel electrophoresis have attracted much attention since the introduction of (agarose) pulsed field technologies by Schwartz and Cantor in 1984 [1]. On one hand, this technology is of foremost importance in biochemistry and in the human genome project. On the other hand, the many subtle effects observed in these systems, such as field inversion gel electrophoresis (FIGE) [2] or band-inversion [3], have forced physicists to go beyond the simple reptation model [4]. In fact, a global model is yet to be suggested. An outstanding technical problem is DNA sequencing. The limits of this technology have not evolved much since 1984, although it is apparently very similar to agarose gel electrophoresis where pulsed fields have had a remarkable impact. However, many differences exist and it is not clear at this time how the present method can be improved by using simple tricks [5]. A new idea was suggested by Ulanovsky, Drouin and Gilbert [6]; see Fig. 1. To slow down and hence increase the separation of the largest molecules, they attached a neutral globular protein, streptavidin, to the end of the DNA molecules. The radius of the gel pores and of the streptavidin being approximately equal, the "tadpole-like" streptavidin-DNA (S-DNA) complex gets "trapped" periodically and must move backward, against the field, to progress further. The electric force on the molecule being proportional to the molecular size M of the DNA, one expects that the velocity $V(M)$ will decrease rapidly with M as larger molecules will find it more difficult to thermally "detrap". The experimental results [6] indeed show an exponential-like decrease of $V(M)$. Because this decrease was too sharp for practical applications, however, the trapping-detrapping process had to be controlled using FIGE pulses [2, 6].

Two other problems make their suggestion [6] difficult to use: the electrophoretic bands tend to broaden very rapidly and $V(M)$ sometimes appear to be time-dependent (G. Drouin, unpublished results). Since pulsed fields do not seem to be efficient with standard sequencing conditions [7–10], the idea of Ulanovsky, Drouin and Gilbert [6] remains one of the most promising ways to increase the approximate 500 base limit of existing sequencers.

Défontaines and Viovy [4, 11, 12] have presented an analytical model of the electrophoretic migration of S-DNA complexes that was based on a slightly modified version of the biased reptation model (BRM) [13]. Their model

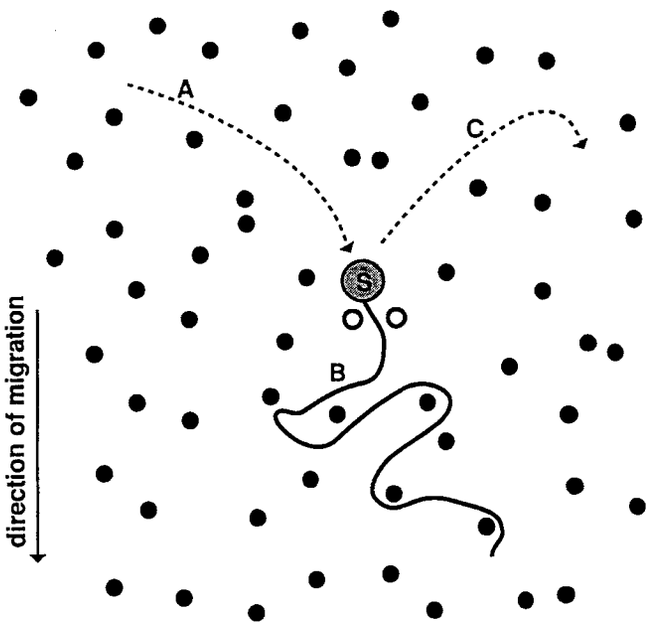

Figure 1. Schematic two-dimensional view of an S-DNA complex during electrophoresis. The dots represent the gel fibers. After having followed corridor A, the molecule is trapped in B because the streptavidin is too large to migrate between the two hollow fibers. The molecule has to move backwards in order to free itself from this trap (*i.e.* to engage in a new, wider corridor C) and progress further in the direction of net migration.

Correspondence: Dr. Gary W. Slater, Department of Physics, University of Ottawa, 150 Louis Pasteur, Ottawa, Ontario, Canada K1N 6N5 (Tel: 613-562-5800, xt. 6775; Fax: 613-562-5190, e-mail:gary@physics.uottawa.ca)

Abbreviations: BRM, biased reptation model; **FIGE,** field inversion gel electrophoresis; **S-DNA,** streptavidin-DNA complex; **TE,** trapping electrophoresis

Keywords: Gel electrophoresis / DNA sequencing / Trapping electrophoresis / Reptation model / Streptavidin

* Now at: Department of Physics, McGill University, Montréal, Québec, Canada, H3T 2T8

0173-0835/95/0505-0704 $5.00+.25/0

indeed predicts a very quick decrease of the mobility past a critical field-dependent molecular size, M^*, in good qualitative agreement with the experimental results reported by [6]. Slater and Villeneuve [14] studied the problem using a computer simulation algorithm based on the BRM. Their results show a similar exponential-like decrease of the mobility, but also a catastrophic increase of the diffusion coefficient. In the limit where the model of Défontaines and Viovy [4, 11, 12], which contains intramolecular stretching modes, reduces to the simulation of Slater and Villeneuve [14], the analytical model does not agree with the simulation results, the latter showing a much faster decrease of the mobility when the molecular size and/or the field intensity are increased. Finally, Desruisseaux and Slater [15] recently showed, using the simulation approach of Slater and Villeneuve [14], that strong steric trapping of S-DNA leads to anomalous transport behavior where the mean electrophoretic band position and variance do not increase linearly with time; in fact, their results suggest that it might be impossible to reach the steady-state in many realistic cases.

In this paper, we present an alternative analytical model of S-DNA trapping electrophoresis (TE). The model is also based on the BRM because it is the only model that leads to tractable equations and analytical results. Moreover, the BRM was shown to be adequate to describe the sequencing of DNA under normal conditions [16]. Our model treats the detrapping process using a diffusion equation with special boundary conditions. This allows us to obtain results that can be used to understand the effects of weak trapping. Moreover, we calculate the diffusion constant and show that it increases exponentially with molecular size; of course, this greatly restricts the usefulness of S-DNA trapping electrophoresis when used with constant fields. Finally, we show quantitatively that it is the random nature of the trapping/detrapping cycles that leads to the highly anomalous transport properties reported by Desruisseaux and Slater [15].

2 Theory

2.1 The Défontaines and Viovy [4, 11, 12] results

In the limit where the polyelectrolyte is not extensible, *i.e.* assuming that the BRM's reptation tube is of fixed length L_0, the Défontaines and Viovy model predicts that the average detrapping time $\tau_d(\varepsilon, N)$ is given by [11, 12]:

$$\frac{\tau_d(\varepsilon, N)}{\tau_B(N)} = \frac{\langle \tau_d(\varepsilon, N, h_x)\rangle}{\tau_B(N)} \propto \left\langle \frac{h_x^2}{a^2}\right\rangle^{1/4} \exp\left[\left\langle \varepsilon N \frac{h_x^2}{4a^2}\right\rangle^{1/2}\right] \quad (1)$$

where N is the number of reptation segments (which is proportional to the molecular size M of the DNA), $a = L_0/N$ is the average pore size of the polyacrylamide gel, h_x is the end-to-end distance of the DNA molecule in the field direction (x), $\varepsilon = qEa/2k_BT$ is the scaled electric field intensity (with E the field intensity and q the net charge per reptation segment); finally, $\tau_B(N) = a^2/2D_S(N)$ is the Brownian time related to the curvilinear diffusion coefficient $D_S(N) = k_BT/\xi(N+\alpha)$, where ξ is the friction coefficient per DNA segment and α is streptavidin's relative friction coefficient (α is of order one; P. Mayer and G. Drouin, unpublished results). The averages noted by the brackets $\langle \ldots \rangle$ mean that we must average over all possible molecular conformations, *i.e.* over the distribution function for the end-to-end distances h_x. For a random conformation with $\langle h_x^2\rangle = {}^1/_3\ Na^2$, Eq. (1) gives

$$\tau_d(\varepsilon, N) \propto N^{5/4}\, e^{[\varepsilon N^{3/2}/\sqrt{12}]} \quad (2)$$

These calculations assume that the fraction f of the pores that can actually trap the streptavidin is very small, *i.e.* $f \ll 1/N$. In this case, traps are well separated. The migration of the S-DNA complex is then composed of well-defined trapping-detrapping cycles and the net mobility is given by

$$V(\varepsilon, N) = \frac{V_0(\varepsilon, N)\ \tau_0(\varepsilon, N)}{\tau_d(\varepsilon, N) + \tau_0(\varepsilon, N)} \quad (3)$$

where τ_0 is the mean time between trapping events and V_0 is the velocity between traps. Equation (3) simply takes into account the time "lost" in the traps. Using Eqs. (2) and (3), Défontaines and Viovy predict that in the limit where the molecule is not extensible, the electrophoretic velocity should decrease asymptotically as $V \propto \exp[-\varepsilon N^{3/2}/(12)^{1/2}]$, in qualitative agreement with the experimental results of [6]. The [4, 11, 12] model also leads to a variety of other interesting regimes when the molecule stretches in response to the electric field (this corresponds to a tube of increased contour length, $L > L_0$). However, Eq. (1) is not valid in the limit where the field intensity is so low that detrapping occurs mostly through normal diffusion [12]. In this article, we assume that the field intensity is low and that the molecule does not stretch (in the jargon of the reptation model, we assume that the tube length $L_o = Na$ is constant). We will also carry out the averages over the distribution of end-to-end distances h_x in a way that is fundamentally different from [4, 11, 12]. Finally, we will calculate the diffusion constant as well as the mobility of the S-DNA complexes since DNA sequencing requires both well-separated and sharp bands (*i.e.* large resolution factors).

2.2 The detrapping process

In the BRM (see [3, 4, 13] for a more detailed description of the BRM), the motion of the DNA molecule is restricted to a "reptation tube" which is formed by the constraints of the gel, *i.e.* the gel fibers. The longitudinal (*i.e.*, along the tube axis) velocity of the DNA molecule is given by

$$V_{tube}(\varepsilon, N, h_x) = \frac{\varepsilon\, h_x}{\tau_B(N)} \quad (4)$$

We note that V_{tube} is a function of the instantaneous value of the end-to-end projection h_x. Therefore, it fluctuates rapidly with time. This expression does not

include the intramolecular (*i.e.* intra-tube) stretching effects considered by [4, 11, 12]. The longitudinal force keeping the molecule inside the trap is

$$F_{trap} = \xi\,(N+\alpha)\,V_{tube} = \frac{\varepsilon\,\xi(N+\alpha)\,h_x}{\tau_B\,(N)} \qquad (5)$$

This force is a function of the end-to-end distance $h_x(t)$ and the different traps may thus have very different "depths" depending on the value of $h_x(t)$. This is similar to diffusion (and drift) in an environment of traps with a random distribution of depths.

Figure 2 shows a possible detrapping scenario where the molecule moves tail first in the field direction to form a pulley-like system. Note that the molecule will often move backward for a while before getting totally trapped again at the same position, but with a different conformation; this will most likely tend to increase the value of h_x as a function of time. In [4, 11, 12], Eq. (2) was obtained for the mean detrapping time $\tau_d(h_x)$, where h_x is the end-to-end distance of the molecule when it gets trapped for the first time, using Kramer's equation and the detrapping scenario shown schematically in Fig. 2.

In our model we assume that h_x remains constant during detrapping as shown schematically in Fig. 3. We use this approximation for two reasons: (i) it makes the problem mathematically tractable; (ii) since the streptavidin is uncharged, there is no reason to assume that the latter will automatically move in the field direction during the detrapping process, as required by the scenario shown in Fig. 2. However, both approaches neglect the fluctuations of h_x during the detrapping process. These fluctuations may play a major role but make the problem difficult to treat analytically.

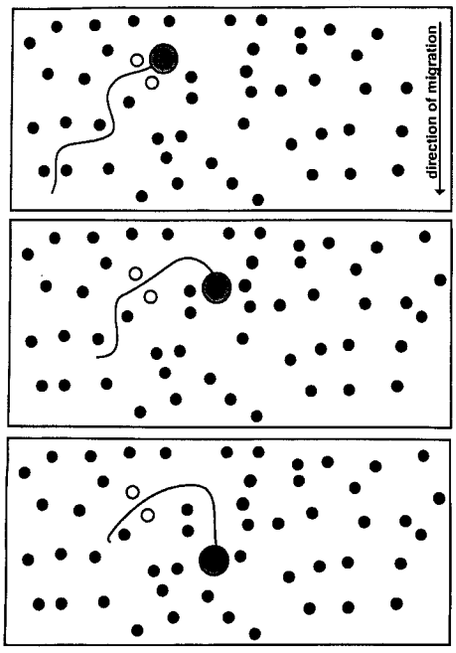

Figure 2. The molecule moves backward, against the field; detrapping is successful when the molecule has disengaged entirely from the narrow bottleneck represented by the grey fibers. During this process, the molecule may get trapped again, in a (slightly) different conformation.

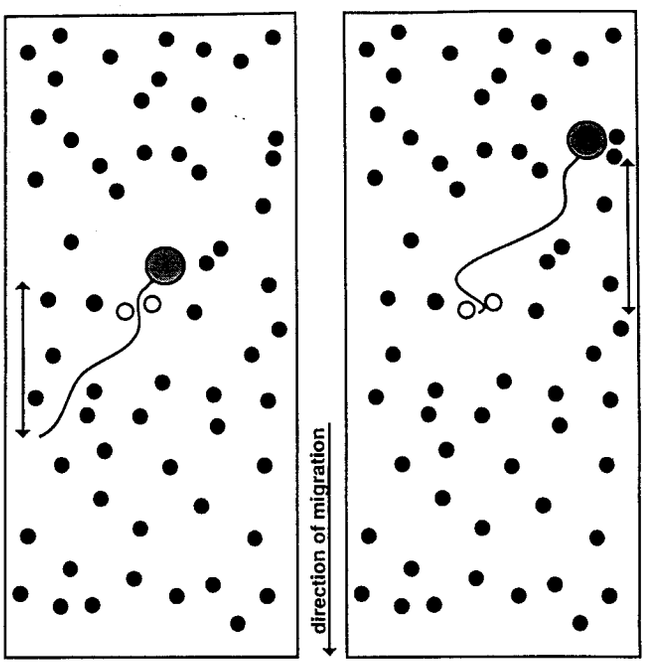

Figure 3. In this article, we assume that the end-to-end distance remains constant during detrapping, as shown by the arrow, to make the calculation of the mean detrapping time tractable.

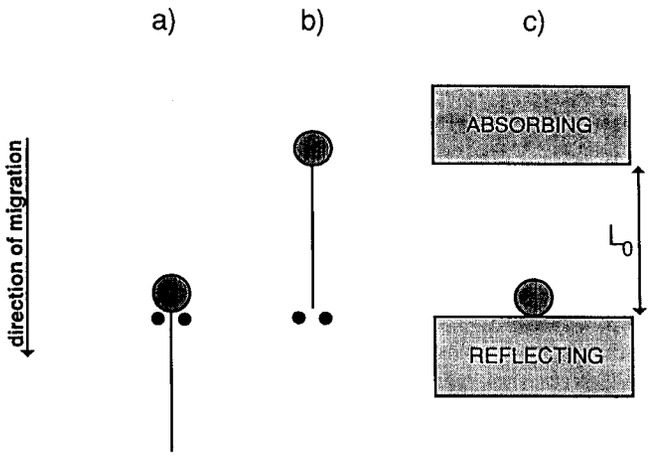

Figure 4. (a) Schematic representation of a molecule at the beginning of the detrapping process; this molecule is "reflected" by the trap when it tries to move downward. (b) The same molecule at the end of the detrapping process; the molecule is "absorbed" out of the trap and can now continue to migrate. (c) The schematic representation of a similar problem: a particle located between a reflecting (the trap) and an absorbing (the freedom) wall.

2.3 The detrapping time

If we assume that the molecule detraps following the scenario describes in Fig. 3, the problem of the chain in its tube becomes similar to the one-dimensional (along the tube axis) problem of a particle on a reflecting wall at s = 0 (the trap) trying to reach an absorbing wall at $s = -Na = -L_0$ (the freedom) while having a constant velocity $(\partial s/\partial t)_{t=0} > 0$ given by Eq. (4) and a diffusion constant $D_s(N) = k_B T/\xi(N+\alpha)$; see Fig. 4. The "diffusion" equation for the mean first-passage or absorbtion time (detrapping time) $\tau_d(s)$ of this process can be written as:

$$D_s \frac{\partial^2 \tau_d(s)}{\partial s^2} + s'(0) \times \frac{\partial \tau_d(s)}{\partial s} + 1 = 0 \quad (6)$$

where s is now the initial position of the particle between the two walls. Note that the velocity $s'(0) = (\partial s/\partial t)_{t=0}$ remains constant (equal to its value at $t = 0$) because of our simplifying assumption that h_x does not change during the detrapping process. The boundary conditions are

$$\left(\frac{\partial \tau_d(s)}{\partial s}\right)_{s=0} = 0 \quad (7)$$

$$\tau_d(s = -L) = 0 \quad (8)$$

The solution to Eqs. (6–8) is given by

$$\tau_d(s) = -\left(\frac{L_o + s}{s'(0)}\right) + \frac{D_s}{s'^2(0)} \times (e^{L_o s'(0)/D_s} - e^{-s\,s'(0)/D_s}) \quad (9)$$

Equation (7) describes the fact that the particle (molecule) is reflected (gets trapped again) when it reaches the wall at $s = 0$ (the streptavidin encounters the same bottleneck again). Equation (8) describes the absorbtion of the particle by the absorbing wall, *i.e.* the termination of the detrapping process.

For the initial conditions $s = 0$ (which defines the beginning of the trapping event), $h_x > 0$, and the curvilinear velocity given by Eq. (4), we obtain, from Eq. (9):

$$\frac{\tau_d(\varepsilon, N, h_x)}{\tau_B(N)} = -\frac{N a}{\varepsilon h_x} + \frac{a^2}{2\varepsilon^2 h_x^2} \times (e^{2\varepsilon N h_x/a} - 1) \quad (10)$$

This mean detrapping time is for a fixed value of h_x, as described before (see Fig. 3). The leading (exponential) term is similar to the one in Eq. (1), but the remainder of the expression is different. In particular, we note that this equation has the right zero-field limit:

$$\lim_{\varepsilon \to 0} \tau_d(\varepsilon, N, h_x) = N^2 \tau_B(N) \propto N^2 (N + \alpha) \quad (11)$$

This is the reptation result with an extra α due to the presence of the streptavidin. Our approach has thus led to a detrapping time that can be used even in the weak-trapping limit. In the next section, we will calculate the average of this detrapping time over the variable h_x in order to calculate both the steady-state velocity and the diffusion coefficient of the S-DNA complex.

It is also possible to calculate the variance $\Delta\tau_d^2(\varepsilon, N, h_x)$ of the mean square detrapping time (Appendix A):

$$\frac{\Delta\tau_d^2(\varepsilon, N, h_x)}{\tau_B^2(N)} = \frac{N^4}{4\lambda^4} \times [e^{4\lambda} + 4e^{2\lambda} - 5 - 4\lambda - 8\lambda e^{2\lambda}] \quad (12)$$

where $\lambda = N\varepsilon h_x/a > 0$. We will see later that the standard deviation of the mean detrapping time is in fact comparable to $\tau_d(\varepsilon, N, h_x)$ itself. This will play an important role.

3 Result

For a given molecular size N, one has

$$N^2 \leq \frac{\tau_d(\varepsilon, N, h_x)}{\tau_B(N)} \leq \frac{e^{2N^2\varepsilon}}{2\varepsilon^2 N^2} \quad (13)$$

Since $N \simeq 2$–20 and $\varepsilon \simeq 0.3$–3.0 represent typical values for DNA sequencing on polyacrylamide gels [16], the upper bound is much larger than the lower bound. Moreover, if we replace h_x by the zero-field value $\langle h_x^2 \rangle^{1/2} = (Na^2/3)^{1/2}$ in Eq. (10), we get the "typical" detrapping time, *i.e.* the detrapping time for a molecule having the (unperturbed) mean end-to-end distance; this time is much shorter than the upper bound in Eq. (13). Therefore, there is a very broad (although not infinitely so) distribution of detrapping times τ_d. This latter remark has three consequences: (i) one must be careful when averaging Eq. (10) over the possible values of h_x because the large values of h_x have a large influence; (ii) the largest relevant detrapping time may exceed the experimental time, in which case one may not be able to reach a steady state; (iii) the trapping/detrapping cycles suffer from a large amount of disorder, *i.e.* the range of possible detrapping times is much larger than the mean detrapping time. These three factors and their impact on the dynamics of S-DNA will be discussed in detail below.

3.1 The averages

As mentioned above, the large values of h_x play an important role in the dynamics of the S-DNA complex because the detrapping time $\tau_d(\varepsilon, N, h_x)$ increases exponentially rapidly with h_x. Therefore, replacing h_x by its mean value in Eq. (10) is not a good approximation. Instead, we suggest the following approach. The only cases of interest are those for which the mean velocity is not negligible, *i.e.* the case where the mean detrapping time is not too large. This is the case only if the argument of the exponential in Eq. (10) is small. Clearly, this requires that the end-to-end distance h_x remains as small as possible, *i.e.*, we must avoid the type of molecular orientation that is typical of gel electrophoresis. As mentioned by Défontaines and Viovy, DNA molecules remain in random-walk conformations if (approximatively) $\varepsilon < 3/\sqrt{N}$, which is thus the only relevant case. Computer simulations [14] indeed showed that oriented molecules have negligible velocities. Therefore, we will take the average of Eq. (10) over an unbiased Gaussian distribution function for the end-to-end distance h_x:

$$p(h_x) \propto \exp - \left(\frac{3 h_x^2}{2Na^2}\right) \quad (14)$$

Although this is a reasonable approach from a physical point of view, it also allows us to obtain simple analytical results. Note that only $h_x > 0$ correspond to traps; therefore, the average of a function $f(h_x)$ is defined as

$$\langle f(h_x) \rangle = \frac{\int_0^\infty f(h_x)\, p(h_x)\, dh_x}{\int_0^\infty p(h_x)\, dh_x} \quad (15)$$

For small molecular sizes such that $\Lambda \equiv (2\ N)^{3/2}\varepsilon < 1$, we can replace the exponentials of Eq. (10) and Eq. (12) by their series expansions to get

$$\frac{\tau_d(\varepsilon, N)}{N^2\,\tau_B(N)} = \frac{\langle \tau_d(\varepsilon, N, h_x)\rangle}{N^2\,\tau_B(N)} \approx 1 + \frac{\Lambda}{\sqrt{27\pi}} + \frac{\Lambda^2}{72} + \ldots \quad (16)$$

$$\frac{\Delta\tau_d^2(\varepsilon, N)}{N^4\,\tau_B^2(N)} = \frac{\langle \Delta\tau_d^2(\varepsilon, N, h_x)\rangle}{N^4\,\tau_B^2(N)} \approx \frac{2}{3} + \frac{8\ L}{15\sqrt{3\pi}} + \frac{11\,\Lambda^2}{270} + \ldots \quad (17)$$

In the limit where $5 < \Lambda < (9N/2)^{1/2}$, we simply obtain

$$\frac{\tau_d(\varepsilon, N)}{N^2\,\tau_B(N)} = \frac{\langle \tau_d(\varepsilon, N, h_x)\rangle}{N^2\,\tau_B(N)} \approx \left(\frac{12}{\Lambda^2}\right)^2 \exp\left(\frac{\Lambda^2}{12}\right), \quad (18)$$

$$\frac{\Delta\tau_d^2(\varepsilon, N)}{N^4\,\tau_B^2(N)} = \frac{\langle \Delta\tau_d^2(\varepsilon, N, h_x)\rangle}{N^4\,\tau_B^2(N)} \approx 8\left(\frac{3}{\Lambda^2}\right)^4 \exp\left(\frac{\Lambda^2}{3}\right) \quad (19)$$

For $\Lambda > (9N/2)^{1/2}$, which corresponds to $N\varepsilon > 3/4$, the large values of h_x (*i.e.* $h_x \approx N$) dominate in the integrals and the Gaussian distribution function becomes useless. However, it turns out that, in this very case, one cannot assume anymore that the contour length L of the reptation tube remains constant. Instead, Eq. (21a) of [12] indicates that if $h_x \approx N$, $N\varepsilon > 1/2$ and $\alpha \approx 1$, one has $L > Na$ and the tube stretches. Therefore, we will not study this limit in this article.

Equations (16) and (17) show that the effect of the field is only a perturbation for small sizes such that $\Lambda < 1$, while Eqs. (18) and (19) indicate that field-induced trapping clearly dominates the dynamics for $\Lambda > 5$. In the latter case, we note that $\tau_d(\varepsilon, N) \propto \exp(2N^3\varepsilon^2/3)$; therefore Eq. (18) tells us that $\tau_d(\varepsilon, N)$ is increasing much more rapidly with size molecular (N) than predicted by Eq. (2). This is because $\langle \exp(h_x/a)\rangle \gg \exp(\langle h_x\rangle/a)$. Although the predicted decrease of $V(N)$ is much steeper (using Eq. 3), the crossover between the small and large trapping regimes is still found for a critical molecular size given roughly by $N^* \propto \varepsilon^{-2/3}$, as obtained by [11, 12]. Finally, we remark that $(\Delta\tau_d^2)^{1/2}$ becomes larger than τ_d when Λ increases; this means that we can have a very broad distribution of detrapping times in this system (to be discussed later).

3.2 The weak trapping limit

With a concentration of traps $f \ll 1/N$, the chain must move over a mean curvilinear distance $d_0 \approx a/f$ along its tube axis before getting trapped. Since the chain has a curvilinear velocity V_{tube} given by Eq. (4), the mean time between traps, due to the field-driven motion of the chain, is

$$\tau_0(\varepsilon, N) \cong \frac{d_0}{\langle V_{tube}\rangle} \cong \frac{\tau_B(N)}{f\varepsilon\langle |h_x/a|\rangle} \cong \frac{\tau_B(N)}{f\varepsilon\sqrt{2N/3\pi}} \quad (20)$$

where we assumed, as before, that the chain keeps a random-walk conformation with $\langle |h_x|\rangle \approx (2N/3\pi)^{1/2}$. The low field regime is found when the inter-trap time is larger than the detrapping time. Using $\tau_d \approx N^2\tau_B(N)$, as suggested by Eq. (16) in this limit, we thus find that $\tau_d/\tau_0 \approx fN\Lambda/(12\pi)^{1/2}$. Since $fN \ll 1$ here, we see that the detrapping time is always small compared to the time it takes to migrate between traps in the low field limit where $\Lambda < 1$. We can then rewrite Eqs. (3) and (16) as

$$\frac{V_0(\varepsilon, N) - V(\varepsilon, N)}{V_0(\varepsilon, N)} \cong \frac{fN\Lambda}{\sqrt{12\pi}} \propto fN^{5/2}\varepsilon \ll 1 \quad (21)$$

Equation (21) shows that although the relative change in velocity is strongly molecular-size-dependent, it is too weak in magnitude to be of any practical use.

3.3 The strong trapping limit

Strong trapping occurs when the detrapping time becomes much larger than the drift time between two traps, *i.e.* when $\tau_d \gg \tau_0$. Since this can happen only when $\Lambda \gg 1$, Eqs. (3), (18) and (20) then give

$$\frac{V}{V_0} \cong \frac{\sqrt{3\pi}\,\Lambda^3}{72fN}\exp\left(-\frac{\Lambda^2}{12}\right) \propto \frac{\varepsilon^3 N^{7/2}}{f}\exp\left(-\frac{2N^3\varepsilon^2}{3}\right) \quad (22)$$

We thus predict a velocity that decreases quickly with molecular size N and field intensity ε. The exponential dependence is in qualitative agreement with the experimental results of [6]. The argument of the exponential is actually the square of the argument of the exponential decrease predicted by [4, 11, 12], which seems to be in better agreement with the simulation results of [14].

In the steady-state, the diffusion constant for a strong trapping regime is given by [17]

$$D = \frac{V^3\langle \Delta\tau_d^2\rangle}{2\,d_0} \quad (23)$$

where $d_0 = V_0\tau_0$, the distance between traps, is a function of gel concentration (through, *e.g.*, the parameter f). In absence of traps, the electrophoretic velocity and the diffusion coefficient for the migrating DNA molecules, in the $\Lambda > 1$ and $N\varepsilon^2 < 1$ limits of interest here, are given by [18]:

$$D_0 \cong \frac{a^2}{6\,\tau_B} \times \varepsilon\sqrt{2N/3\pi} \quad (24)$$

$$V_0 = \frac{\varepsilon\,a}{3\tau_B} \quad (25)$$

Using Eqs. (19), (22), (23), (24) and (25), we then find:

$$\frac{D}{D_0} = \left(\frac{\pi}{192}\right)^{3/2}\frac{\Lambda^3}{f^2N^2}\exp\left(\frac{\Lambda^2}{12}\right) \propto \frac{\varepsilon^3 N^{5/2}}{f^2}\exp\left(\frac{2N^3\varepsilon^2}{3}\right) \quad (26)$$

Of course, an exponential decrease of the velocity, as given by Eq. (22), together with an exponential increase of the diffusion coefficient, as given by this last equation, means that the number of molecules effectively separated is diminished. Also noteworthy is that our results predict that the diffusion coefficient will start increasing before (*i.e.* for smaller molecules) the velocity starts to decrease, as observed by [14] (due to the prefactors in each expression).

We thus conclude that the experimental results of [6] can indeed be explained qualitatively by the type of trapping suggested by these authors, and that constant fields cannot lead to improved DNA sequencing because of the large diffusion generated by the random detrapping process.

3.4 The transient regime

We now return to the effect of the large dispersion $< \Delta\tau_d^2 >$. We first note that in the strong trapping limit, one has

$$\frac{\Delta\tau_d}{\tau_d} \cong \frac{\sqrt{2}}{8} \exp\left(\frac{\Lambda^2}{12}\right) \gg 1 \tag{27}$$

This broad distribution of detrapping times is typical of trapping in disordered systems [19]. Here, we have a unique case: the disorder is provided by the broad distribution of end-to-end distances h_x since it is this parameter which measures the "depth" of the trap. Therefore, it is essentially a case of self-inflicted disorder.

In order to examine the consequences of this broad distribution, we will study the distribution $p(\tau_d)d\tau_d$ for the mean detrapping time $\tau_d(h_x)$. We can calculate this function as

$$p(h_x)\, dh_x = \frac{p(h_x(\tau_d))}{d\tau_d/dh_x}\, d\tau_d = p(\tau_d)\, d\tau_d \tag{28}$$

where $p(h_x)$ is given by Eq. (14), $d\tau_d/dh_x$ can be obtained by taking the derivative of Eq. (10), and $h_x(\tau_d)$ must be obtained by inverting Eq. (10). For simplicity, this approach neglects the distribution of detrapping times $\tau_d(h_x)$ for a fixed value of h_x, although those were included in Eq. (19). Inverting Eq. (10) cannot be accomplished analytically; therefore, we must rely on numerical methods.

Figure 5 shows the distribution function $p(\tau_d)$ for different values of the parameter $\Lambda = (2N)^{3/2}\,\varepsilon$. It is remarkable that we almost have a power-law distribution of the type

$$p(\tau_d) \sim \frac{1}{\tau_d^{1+\mu}} \tag{29}$$

over a large range of detrapping times. The exponent μ falls approximately in the following ranges:

$$2 < \mu \quad \text{if} \quad \Lambda < 7 \tag{30}$$

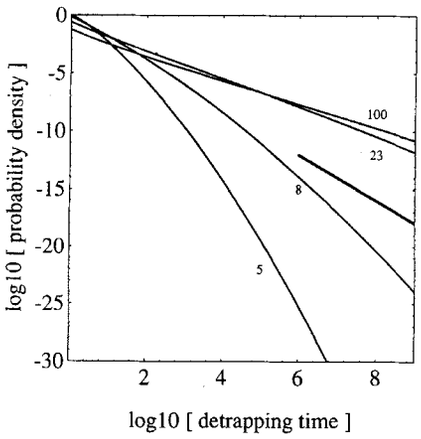

Figure 5. Probability density $p(\tau_d)$ *vs.* detrapping time τ_d for different values of Λ (from bottom to top: 5, 8, 23 and 100). The straight line plotted on the figure has a slope of −2 (corresponding to a value of $\mu = 1$; we obtain transient regimes for both the mean position $\langle x(t) \rangle$ and the dispersion $\langle \Delta x^2(t) \rangle$ when $\mu < 1$). Times are in arbitrary units.

$$1 < \mu < 2 \quad \text{if} \quad 7 < \Lambda < 11 \tag{31}$$

$$0 < \mu < 1 \quad \text{if} \quad \Lambda > 11 \tag{32}$$

We note that the exponent μ decreases when Λ increases. Of course, these numbers are somewhat approximative since the decay is not exactly a power-law. Our calculation of the distribution function is valid only when the Gaussian distribution function (14) is valid, *i.e.* when h_x is not too large compared to $Na^{1/2}$; for larger values of h_x, and hence τ_d, the distribution function should decrease much faster than predicted here. According to Eq. (10), this means that the power-law-like decay is valid for detrapping times lower than approximately

$$\frac{\tau_d}{\tau_B} < \frac{N^2}{\Lambda}\, e^{\Lambda} \tag{33}$$

For longer times, the decay should be much more rapid. According to the theory of anomalous diffusion [19], a trapping process with a slow decaying tail like the one given by Eq. (29) leads to anomalous transport phenomena where the mean position $\langle x(t) \rangle$ and the mean variance $\langle \Delta x^2(t) \rangle$ (of the electrophoretic band) will follow the power laws

$$\langle x(t) \rangle \sim t^1; \quad \langle \Delta x^2(t) \rangle \sim t^1 \quad \text{if } \mu > 2 \tag{34}$$

$$\langle x(t) \rangle \sim t^1; \quad \langle \Delta x^2(t) \rangle \sim t^{2/\mu} \quad \text{if } 2 > \mu > 1 \tag{35}$$

$$\langle x(t) \rangle \sim t^{\mu}; \quad \langle \Delta x^2(t) \rangle \sim t^{2\mu} \quad \text{if } 1 > \mu > 0 \tag{36}$$

The reason for this anomalous behavior is simple: when the distribution function for detrapping times τ_d decays slowly, the particle often falls into a trap whose detrapping time is larger than the total time since the beginning of the migration. In this case, it is the last deep trap that dominates the dynamics of the system and the mean position and peak dispersion are directly related to the exact shape of the tail of the distribution function $p(\tau_d)$. For example, we can show [15] that, in the $1 > \mu > 0$ regime, the mean position of the particles is given roughly by

$$\langle x(t)\rangle \sim \left[\int_{t}^{\infty} p(\tau_d)\, d\tau_d\right]^{-1} \quad (37)$$

if $\tau_0 \ll \tau_d$. For a power-law decay as given by Eq. (29) above, this reduces to Eq. (36). Figure 6 shows how $\langle x(t)\rangle$ scales with time t when Eqs. (28) and (37) are solved numerically for $\Lambda = 23$. For a normal situation, we would observe a line of slope unity (*i.e.* $\langle x(t)\rangle \propto t^1$). Here, we find instead that $\langle x(t)\rangle \propto t^{0.3}$ over many decades. Normal behavior is eventually reached (but, as explained before, our Gaussian distribution function is not reliable in this region because it overestimates the importance of the longest detrapping times of the tail of the distribution function). These theoretical results are in fair agreement with our recent simulation results [15]. For $N = 30$ and $\varepsilon = 0.05$, which corresponds to $\Lambda \approx 23$, Descruisseaux and Slater [15] indeed found a long-lasting anomalous transient regime, in agreement with Eq. (36), with $\mu = 0.65$ and a steady-state time $\approx 10^{10}\ \tau_B$ beyond which the anomalous effects disappeared. Equation (33) predicts that the anomalous regime should end for times $\approx 10^{11}\ \tau_B$. Those results are in fair agreement with the simulation results if we consider the numerous approximations that we had to make in order to obtain analytical results.

In conclusion, the unique trapping process of the S-DNA complexes leads to highly anomalous transport properties in the limit where the velocity becomes strongly molecular-size-dependent. These anomalous regimes last for a very long time and are characterized by slow drift and fast dispersion, *i.e.* by a loss of resolution. Together with the increased diffusion coefficient one has in the steady-state, these anomalous effects make constant fields unlikely to be of any use in increasing the performance of DNA sequencing systems. One must indeed reduce the importance of trapping in order to get useful results, as was already remarked by [6]. A simple approach can be considered: using pulsed fields to help the molecules to detrap. Note that the anomalous regimes found here might remain important if long pulses are used; this will be examined in a future article.

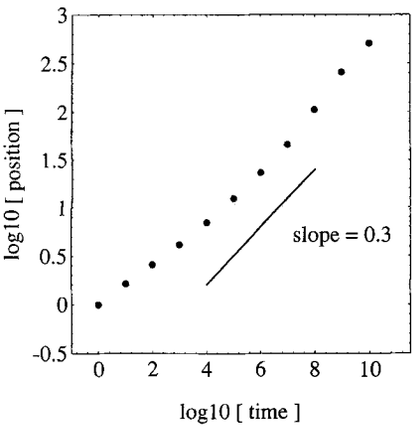

Figure 6. Mean position $< x(t) >$ *vs.* time t when $\Lambda = 23$. We observe that $< x(t) > \propto t^{0.3}$ for intermediate times. Position and time are given in arbitrary units.

4 Discussion

We derived an analytical model of S-DNA gel electrophoresis providing detailed predictions for both the steady-state velocity and the diffusion coefficient. This model, based on a simple diffusion equation, is valid for both the weak and the strong trapping regimes. Moreover, it correctly predicts the existence of a distribution of detrapping time $p(\tau_d)$ (as opposed to a delta peak distribution). This distribution is of foremost importance when calculating band dispersion. Moreover, the tail of the distribution occasionally leads to anomalous transport behavior (observed in previous computer simulations by [15]). Even though we employed a different detrapping mechanism than the one used by Défontaines and Viovy [4, 11, 12], the resulting crossover region retains the same scaling form, namely $N^* \propto \varepsilon^{-2/3}$. However, we showed that the predicted steady-state velocity decreases much more rapidly in the $\Lambda > 5$ (strong trapping) regime. The predicted steady-state diffusion coefficient is shown to increase rapidly with molecular size in the same limit. The last two findings greatly decrease the number of molecules effectively separated. Preliminary computer simulations agree well with all the predictions made in this paper [14–15]. Qualitative comparisons with experimental results are also noticeable: for instance, cases where $\langle x(t)\rangle$ and $\langle \Delta x^2(t)\rangle$ do not scale like t^1 have been observed, although it is too early to attribute this to an anomalous behavior such as predicted here (G. Drouin, unpublished results).

From our computer simulations [15] and this analytical model we conclude that the fast decrease of the steady-state velocity, the fast increase of the steady-state diffusion coefficient, and the anomalous regimes observed for $\Lambda > 5$ can all be explained by a broad (slowly decaying) distribution of detrapping time. In order to obtain higher velocities, Ulanovsky, Drouin, and Gilbert [6] proposed using pulsed fields. This helps the molecules to detrap and it should also reduce the width of the distribution of detrapping times. This predicted behavior has been observed in recent computer simulations [20].

We are now doing experimental work to test the predictions of the analytical model presented in this article. Since no experimental results on TE have been reported since [6], it is important to have experimental confirmations of the quantitative predictions and of the anomalous regimes described before to optimize the performance of TE.

This work was supported by a Strategic Grant from the National Science and Engineering Research Council (NSERC) of Canada to GWS and GD, by an NSERC Research Grant to GWS and by an NSERC Undergraduate University Summer Research Award to CV.

Received October 26, 1994

5 References

[1] Schwartz, D. C., Cantor, C. R., *Cell* 1984, *37*, 67–75.
[2] Carle, G. F., Frank, M., Olson, M. W., *Science* 1985, *232*, 65–68.

[3] Noolandi, J., Rousseau, J., Slater, G. W., Turmel, C., Lalande, M., *Phys. Rev. Lett.* 1987, *58*, 2428–2431.
[4] Défontaines, A.-D., Viovy, J.-L., in: Burmeister, M., Ulanovsky, L. (Ed.), *Pulsed-Field Gel Electrophoresis, Protocols, Methods, and Theories,* The Humana Press, Totowa (NJ), 1992, pp. 403–450.
[5] Slater, G. W., Mayer, P., Drouin, G., *Analusis* 1993, *21*, M25–M28.
[6] Ulanovsky, L., Drouin, G., Gilbert, W., *Nature* 1990, *343*, 190–192.
[7] Lai, E., Davi, N. A., Hood, L. E., *Electrophoresis* 1989, *10*, 65–67.
[8] Brassard, E., Turmel, C., Noolandi, J., *Electrophoresis* 1992, *13*, 529–535.
[9] Heller, C., Beck, S., *Nucleic Acids Res.* 1992, *20*, 2247–2252.
[10] Slater, G. W., Drouin, G., *Electrophoresis* 1992, *13*, 574–582.
[11] Défontaines, A.-D., Viovy, J.-L., in: Cantor, C. R., Lim, M. A. (Eds.), *Proceedings of First International Conference on Electrophoresis, Supercomputer and the Human Genome*, World Scientific, Singapore 1991, pp. 286–313.
[12] Défontaines, A.-D., Viovy, J.-L., *Electrophoresis* 1993, *14*, 8–17.
[13] Slater, G. W., Noolandi, J., in: Lee, L.-H. (Ed.), *New Trends in Physics and Physical Chemistry of Polymers,* Plenum Press, New York 1989, pp. 547–600.
[14] Slater, G. W., Villeneuve, C., *J. Polym. Sci. B* 1992, *30*, 1451–1457.
[15] Desruisseaux, C., Slater, G. W., *Phys. Rev. E* 1994, *49*, 5885–5888.
[16] Mayer, P., Slater, G. W., Drouin, G., *Appl. Theor. Electrophoresis* 1993, *3*, 147–155.
[17] Bouchaud, J.-P., Georges, A., *C. R. Acad. Sci. Paris* 1988, *307*, 1431–1436.
[18] Slater, G. W., *Electrophoresis* 1993, *14*, 1–7.
[19] Bouchaud, J.-P., Georges, A., *Physics Reports* 1990, *195*, 127–293.
[20] Desruisseaux, C., *M. Sc. Thesis,* University of Ottawa, Ottawa 1994.
[21] Gardner, C., *Hand Book of Stochastic Methods for Physics, Chemistry and the Natural Sciences,* Springer-Verlag, Berlin 1983, pp. 118–143.

6 Appendix

In this appendix, we study the Brownian dynamics of the S-DNA molecule inside a trap. We first map this problem onto the mathematical problem of a point-like particle performing a one-dimensional random walk between two walls, one absorbing (this represents the end of the detrapping process, *i.e.* the completion of a jump of length L against the field) and one reflecting (representing the trap itself; see Fig. 4). We present the theoretical analysis (based on the Fokker-Planck equation) leading to our expressions for the mean value of the absorption time τ_d and its variantce $(\Delta\tau_d)^2$.

Let the particle be initially at position s (with $-L \leq s \leq 0$) at time $t = 0$. The absorbing and reflecting walls are at positions $-L$ and 0, respectively; the end of the detrapping process thus happens when $s = -L$ and it starts with $s = 0$.

Let $G(s,t)$be the probability that at time t the particle is still in the interval $]-L, 0]$. It obeys the Fokker-Planck equation [21]

$$\frac{\partial}{\partial t} G(s, t) = D \frac{\partial^2}{\partial s^2} G(s, t) + V \frac{\partial}{\partial s} G(s, t) \tag{A.1}$$

where D and V are the diffusion coefficient and drift velocity of the particle, respectively. In our case, V and D are the curvilinear velocity and diffusion coefficient of the molecule in its tube, respectively. The initial condition is

$$G(s, 0) = 1 \tag{A.2}$$

and the boundary conditions are

$$G(-L, t) = 0 \tag{A.3}$$

$$\left(\frac{\mathrm{d}\, G(s, t)}{\mathrm{d}\, s}\right)_{s=0} = 0 \tag{A.4}$$

Let the time at which the particle is absorbed be T. The mean absorption time $\tau_d(S) = < T >$ is defined by [21]

$$\tau_d(s) = \int_0^\infty G(s, t)\, \mathrm{d}t \tag{A.5}$$

Integrating Eqs. (A.1), (A.3) and (A.4) over t between 0 and ∞, we obtain an ordinary differential equation for $\tau_d(s)$

$$D \frac{\mathrm{d}^2\tau_d(s)}{\mathrm{d}s^2} + V \frac{\mathrm{d}\tau_d(s)}{\mathrm{d}s} = -1 \tag{A.6}$$

with the boundary conditions

$$\tau_d(0) = 0 \tag{A.7}$$

$$\left(\frac{\mathrm{d}\tau_d(s)}{\mathrm{d}s}\right)_{s=0} = 0 \tag{A.8}$$

Solving Eq. (A.6) with these boundary conditions, we find

$$\tau_d(s) = \frac{D\, e^{\frac{VL}{D}} \left(1 - e^{-\frac{Vs}{D}}\right) - Vs}{V^2} \tag{A.9}$$

When the particle starts on the reflecting wall (as is the case for our problem), we have $s = 0$ and

$$\tau_d \equiv \tau_d(0) = \frac{D\, e^{\frac{LV}{D}} - LV - D}{V^2} \tag{A.10}$$

Similarly, we define $\tau_{d,n}(s) = < T^n >$ as

$$\tau_{d,n}(s) = n \int_0^\infty t^{n-1}\, G(s, t)\, \mathrm{d}t \tag{A.11}$$

We see that, by repeated integration, all the moments of the absorbing time can be found from the differential equation:

$$D \frac{\mathrm{d}^2}{\mathrm{d}s^2} \tau_{d,n}(s) + V \frac{\mathrm{d}}{\mathrm{d}s} \tau_{d,n}(s) = -\, n\, \tau_{d,n-1}(s) \tag{A.12}$$

The corresponding boundary conditions are

$$\tau_{d,n}(0) = 0 \tag{A.13}$$

$$\left(\frac{\mathrm{d}\, \tau_{d,n}(s)}{\mathrm{d}\, s}\right)_{s=0} = 0 \tag{A.14}$$

With Eqs. (A.9), (A.13) and (A.14), $\tau_{d,2}(s)$ can be obtained by solving Eq. (A.12) to obtain

$$\tau_{d,2}(s) = \frac{2D\ (2D - 2\ VL - Vs)\ e^{\frac{VL}{D}} + 2D^2\ e^{\frac{2VL}{D}}}{V^4} - \frac{2D\ (2D - 2VL + Vs)\ e^{\frac{V(L-s)}{D}}}{V^4} - \frac{2D^2\ e^{\frac{V(2L-s)}{D}} + Vs\ (2D - Vs)}{V^4} \quad \text{(A.15)}$$

When s = 0, we have

$$\tau_{d,2}(0) = \frac{2D^2\ e^{\frac{2LV}{D}} - 2D(3LV - D)\ e^{\frac{LV}{D}} + (L^2V^2 - 4D^2)}{V^4} \quad \text{(A.16)}$$

The variance of the absorbing time $(\Delta\tau_d)^2 = \tau_{d,2} - (\tau_d)^2$ is thus given by

$$\Delta\tau_d^2 = \frac{D^2\ e^{\frac{2LV}{D}} - 4D\ (LV - D)\ e^{\frac{LV}{D}} - D(2LV + 5D)}{V^4} \quad \text{(A.17)}$$

Equations (A.10) and (A.17), when D and V are replaced by their definitions, correspond to our Eqs. (10) and (12).